



Ultrafast Electron Transfer at Organic Semiconductor Interfaces: Importance of Molecular Orientation

Alexander L. Ayzner,^{†,‡,||} Dennis Nordlund,[‡] Do-Hwan Kim,[§] Zhenan Bao,[†] and Michael F. Toney^{*,‡}

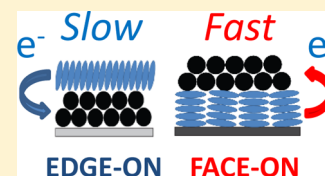
[†]Department of Chemical Engineering, Stanford University, Stanford, California 94305, United States

[‡]Stanford Synchrotron Radiation Lightsource, SLAC National Accelerator Laboratory, Menlo Park, California 94025, United States

[§]Department of Organic Materials and Fiber Engineering, Soongsil University, Seoul, 156-743 Korea

S Supporting Information

ABSTRACT: Much is known about the rate of photoexcited charge generation in at organic donor/acceptor (D/A) heterojunctions overaged over all relative arrangements. However, there has been very little experimental work investigating how the photoexcited electron transfer (ET) rate depends on the precise relative molecular orientation between D and A in thin solid films. This is the question that we address in this work. We find that the ET rate depends strongly on the relative molecular arrangement: The interface where the model donor compound copper phthalocyanine is oriented face-on with respect to the fullerene C₆₀ acceptor yields a rate that is approximately 4 times faster than that of the edge-on oriented interface. Our results suggest that the D/A electronic coupling is significantly enhanced in the face-on case, which agrees well with theoretical predictions, underscoring the importance of controlling the relative interfacial molecular orientation.



Charge transfer in condensed phase systems is a ubiquitous phenomenon that is highly important for a broad range of processes, including catalytic conversion at inorganic surfaces, photosynthesis and photovoltaic power generation. Specifically in solar cells based on conjugated organic materials, photoexcited charge transfer at donor/acceptor (D/A) heterojunction interfaces is the penultimate step for the generation of free charge carriers.¹ Having recently surpassed the 10% power conversion efficiency mark,^{2,3} organic solar cells continue to attract large interest due to their inexpensive processing, light weight, and potential for facile integration into flexible and stretchable devices. One of the factors limiting controlled advances in efficiency is a lack of detailed understanding of charge transfer within these π -conjugated photovoltaic devices. In particular, in order to improve control of energetics and dynamics at all-organic interfaces, an understanding of how the relative molecular orientation affects the intermolecular coupling is essential. This topic is also of fundamental interest to the field of charge transfer.

Although recent studies have provided insight into the dependence of the device photocurrent on molecular orientation,⁴ quantitative experiments that shed light on how the relative D/A orientation affects the interfacial electronic coupling and thus the electron transfer (ET) rate in the thin solid film have not been carried out. It is known from optical pump/probe spectroscopy that photoexcited ET from organic donors to the archetypal acceptor C₆₀ often proceeds on sub-50 fs time scales.⁵ However, it is usually challenging to achieve appropriate ultrafast laser pulses that are short enough to effectively probe such fast dynamics. Moreover, it can be difficult to deconvolute the interface ET dynamics from the overall rate of excitation quenching, which also depends on the rate of diffusion of excitations. Therefore, the ET probe can be more precise if it is

interface-sensitive. Both the time resolution and spatial definition are fulfilled in resonant core-hole spectroscopy, where the decay of core-excited states is used to probe dynamics in energy space.^{6,7} The large excitation energies of core-excitations lead to core-hole lifetimes in the femtosecond regime: about 5 fs for low Z elements like C and N. When evaluating probabilities of charge transfer processes to occur in the time frame of the core-hole lifetime, this translates into a dynamic range of approximately 0.5 to 50 fs for this technique. The excitation of core electrons renders the technique element-specific and local in character, and the escape depth of ejected electrons from the primary Auger decay pathways is on the order of a 10–20 Å, which adds interface sensitivity and specificity when Auger electrons are detected.

In this work, we use the core-hole clock (CHC) implementation of resonant auger electron (RAE) spectroscopy to address the orientation dependence of the interfacial electronic coupling on a femtosecond time scales using a model heterojunction interface. We have chosen an archetypal small molecule D/A pair, where copper(II) phthalocyanine (CuPc) serves as the photoexcited electron donor, and the fullerene C₆₀ is the electron acceptor. In addition to being very well characterized, we chose this pair because (a) the orientation of CuPc can be readily tuned by using surface interactions,⁸ and (b) C₆₀ is quasi-spherical, which means the relative orientation is controlled entirely by the orientation of CuPc. We find that in pure CuPc films, *intramolecular* tunneling delocalizes the photoexcited electron on a sub-50 fs timescale. However, in heterojunction thin films where the CuPc is oriented largely face-

Received: October 24, 2014

Accepted: December 3, 2014

Published: December 4, 2014

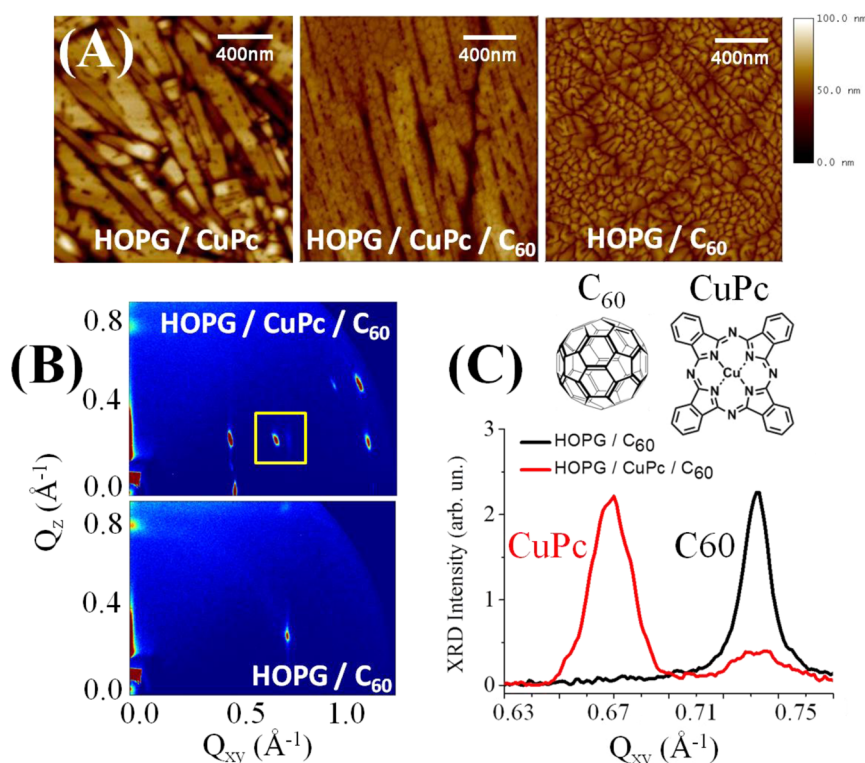


Figure 1. (a) AFM topography images of CuPc (left), CuPc with a C₆₀ overlayer (middle), and C₆₀ (right) thin films deposited onto HOPG. (b) 2D GIXD images for HOPG/CuPc/C₆₀ (top) and HOPG/C₆₀ (bottom). Both images show narrow Bragg peaks corresponding to lateral crystalline coherence lengths between 50 and 60 nm. The scattering pattern of the HOPG/CuPc/C₆₀ bilayer is nearly identical to that of a single-layer CuPc film (not shown) except for a single faint C₆₀ peak. (c) Chemical structures of CuPc and C₆₀ (top), and a 1D line profile across Bragg peaks in the region shown with a yellow box in (b). The black curve (HOPG/C₆₀) corresponds to the brightest peak visible in bottom panel of (b). The red curve shows that in the HOPG/CuPc/C₆₀ sample, there is an additional faint peak next to a bright CuPc Bragg reflection that coincides with the position of the Bragg peak of C₆₀. This shows that the π -stacking interaction with both HOPG and CuPc induces a similar crystal orientation in the C₆₀ film.

on to C₆₀, we also find evidence for additional *intermolecular* electron tunneling to the C₆₀ acceptor on time scales comparable to intramolecular tunneling. We also show that for the same excitation energies, there is little indication of intermolecular electron transfer in the edge-on oriented interface on these ultrafast time scales. Given the energy level alignment at these interfaces, our results imply that the interfacial electronic coupling depends on the relative D/A orientation and is larger in the face-on case.

To template the model bilayer films used in the ET studies, we have grown CuPc and C₆₀ on highly oriented pyrolytic graphite (HOPG), since a graphite surface has been shown to promote face-on growth; we show below that this leads to a primarily face-on arrangement between the two molecules.⁸ The edge-on interface is prepared by first depositing a layer of C₆₀ followed by deposition of a very thin CuPc. Figure 1 shows the structural characterization of our films using both AFM and grazing-incidence X-ray diffraction (GIXD) images. The data show that (a) bilayer films are continuous, and (b) that the GIXD images of CuPc on HOPG are consistent with a face-on arrangement. Additional details are provided in the Supporting Information (SI). The chemical structures of the molecules are shown in Figure 1c.

To get a better understanding of the relative molecular orientation, we have measured the average tilt angle of the CuPc molecular plane relative to the surface normal using angle-resolved near-edge X-ray absorption spectroscopy (XAS) at the nitrogen K-edge (Figure 2). N 1s XA spectra at X-ray incidence angles of 70° and 20° between the incident electric field and the

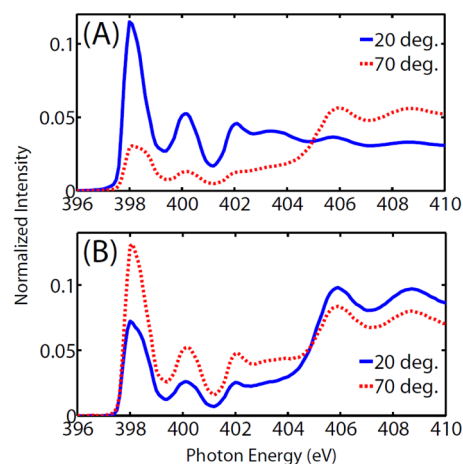


Figure 2. XAS spectra of (a) CuPc/HOPG and (b) C₆₀/submonolayer CuPc at 20 (solid blue line) and 70 (dashed red line) degree incidence. The spectra show qualitative different behavior at different incidence angles for the two different samples, which unambiguously shows that on C₆₀, CuPc is oriented primarily edge-on, whereas when deposited on HOPG, CuPc is primarily face-on with respect to the substrate.

substrate plane are plotted for HOPG/CuPc (Figure 2a) and HOPG/C₆₀(multilayer)/CuPc(submonolayer) (Figure 2b). The sharp peak structure close to the absorption edge up to approximately 402 eV corresponds to N 1s $\rightarrow \pi^*$ transitions, where the final states correspond to (lowest) unoccupied molecular orbitals with significant wave function amplitude on

the two chemically distinct N atoms of CuPc. We emphasize that the element specificity (excitation of N 1s core-level) ensures that we are selectively looking at CuPc *only*, without any contributions from HOPG and C₆₀.

The spectra display a strong dichroism for the characteristic π^* resonances below 402 eV. The angular dependence immediately indicates that CuPc adopts a primarily face-on orientation on HOPG and an edge-on orientation in the submonolayer evaporated on top of C₆₀. Assuming azimuthal averaging and a linear polarization factor of 0.9, we apply a well-established formalism⁹ to extract an average tilt angle of the CuPc molecular plane with respect to the substrate plane of 26° (HOPG/CuPc) and 67° (HOPG/C₆₀/CuPc). These tilt angles are in good agreement with X-ray diffraction data from previous reports: the tilt angle between the molecular plane of CuPc and the substrate when (110) planes of the α -polymorph were oriented normal to the substrate was 26°. ¹⁰ Thus, CuPc deposited on HOPG likely crystallizes as an α -polymorph with the molecular core primarily face-on with respect to the substrate. In contrast, on C₆₀, the α -polymorph is oriented primarily edge-on with respect to the C₆₀ substrate.

Having established that we can form primarily face-on and edge-on CuPc/C₆₀ interfaces, we use the CHC implementation of RAE spectroscopy to answer the following question: Is there a difference in electron transfer dynamics on the sub-100 fs time scale as a function of relative D/A orientation? The ultrafast Auger decay processes that allow us to estimate ET times begin with the excitation of a core electron into an unoccupied state, creating a hole in a core orbital. The core-excited state ($1s \rightarrow \text{LUMO}+n$, $n = 0, 1, \dots$) is an excitonic state. The excitation is relatively local to the core-hole of the absorbing atom, and due to the large excitation energy, decays extremely fast (about 6 fs for C 1s and 5 fs for N 1s).¹¹ For light elements in organic molecules, the main decay pathway following core-ionization or core-excitation is by emission of Auger electrons. The CHC method relies on relating the energetics and intensities of decay processes to the branching ratio of localized and delocalized photoexcited electrons on sub-100 fs time scales, i.e. to the branching ratio of Auger intensities that represent complete localization (with respect to the core-hole) and complete delocalization.

In Figure 3, we schematically show the energetically distinct decay pathways following resonant excitation into a bound excited state ($1s \rightarrow \text{LUMO}+n$).¹² In particular, if the excited electron remains localized until the core-hole decay occurs, it can either participate in recombining with the core hole itself (participator) or remain in the LUMO+ n state (spectator). In the participator decay, the excited electron fills the core-hole, and the excitation energy is transferred to a valence band ($\text{HOMO}-n$, $n = 0, 1, \dots$) electron that is ejected, leaving a final state that is identical to the final state in direct photoemission (photoelectric effect), i.e. one hole in the valence band. This process is referred to as resonant photoemission, or *participator* Auger. When photoionization of the core-excited state occurs into the continuum, the only possible decay channel is akin to spectator Auger but differs in energy from the latter; this process is called *normal* Auger. Since the core-excited state following ET is very similar to one where the photoexcited electron was ejected to the continuum, normal Auger decay is a signature of ultrafast ET, as described in more detail in the SI.

In order to evaluate ultrafast electron transfer dynamics as a function of relative D/A orientation, we investigated CuPc/C₆₀ interfaces in both edge-on and face-on morphologies along with a pure donor film. To perform the decomposition of the total

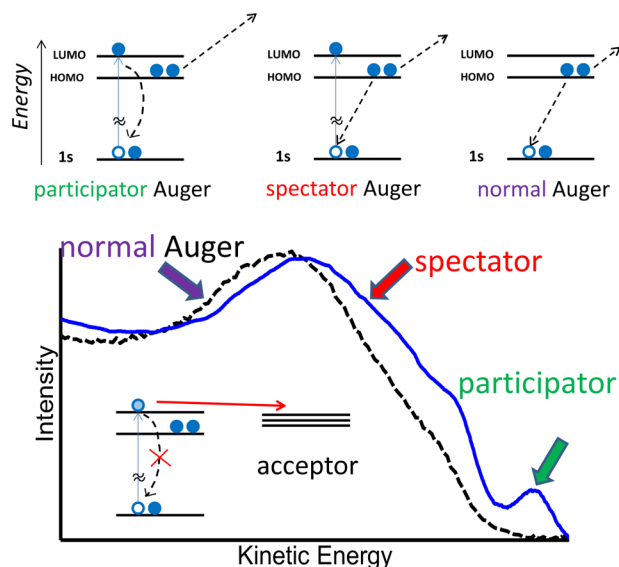


Figure 3. Principles of the CHC method. The top shows the relevant Auger decays following absorption of an X-ray photon, as discussed in the text. The bottom demonstrates the signature of ET. In the no-ET case, the Auger spectrum (blue solid line) shows both the participator and the spectator contributions, the latter shifted from the normal Auger (black dashed line) by the screening energy (spectator shift) due to the presence of the excited electron. When ET competes with the core-hole lifetime, the participator peak (as well as the spectator peak) drop in intensity (to zero in the extreme case). The branching ratio between the normal Auger and spectator + participator Auger intensities can be related to the rate of electron delocalization away from the core-hole. The inset in the plot is a cartoon illustrating that the participator channel shuts off when the photoexcited electron tunnels away from the core-hole.

Auger spectrum into its constituents to calculate the branching ratio we need to identify a “pure resonant” spectrum, i.e., an Auger spectrum that represents complete localization and thus no normal Auger component. We thus first investigated Auger spectra due to the pristine nominally 20 nm thick CuPc film. Figure 4A shows resonant Auger electron spectra (RAES) across the N 1s \rightarrow LUMO XAS absorption resonance for the 20 nm CuPc on HOPG as a function of photon energy in the vicinity of the first XAS peak corresponding to transitions into π^* states.

At several photon energies in the vicinity of the XAS absorption maximum (398 eV) a participator peak is visible, as is a rather distinct spectator shift in the spectator Auger region relative to the normal Auger spectrum (core ionization with 450 eV excitation). The trace at 398 eV indicates a largely localized core-excited state near the absorption edge that does not couple strongly to the environment within the time scales accessible by the CHC. However, the fact that participator Auger disappears at increasing photon energies, and that the spectator spectrum begins to resemble normal Auger, shows that the excited electronic wave function becomes more delocalized relative to the core-hole. Since we have observed this effect in thin films that showed no Bragg diffraction (both on Si and HOPG) and thus likely minimal long-range order, we attribute these spectral changes to a largely intramolecular tunneling process, which has been suggested previously.¹³ A detailed study of state-dependent screening (including photon energy-dependent effects such as coupled electron–phonon dynamics)^{14,15} is beyond the scope of this investigation.

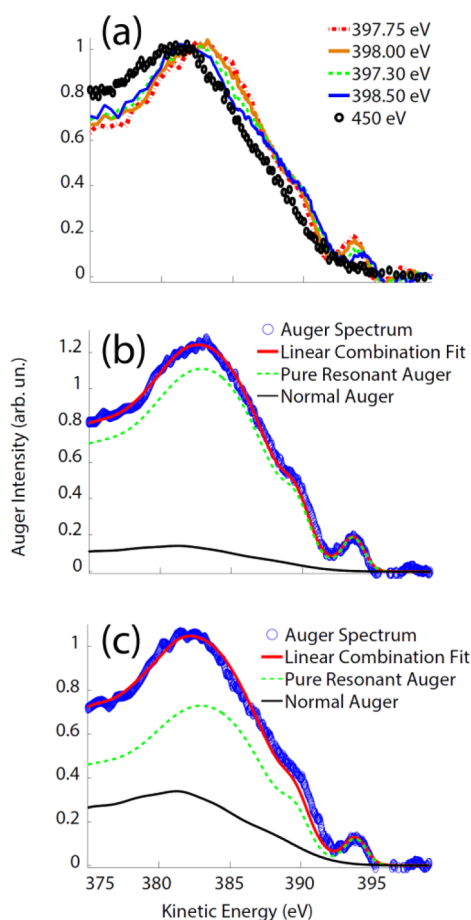


Figure 4. Auger spectra for a neat 20 nm CuPC film on HOPG. (a) excitation at photon energies in the vicinity of the 1st XAS π^* resonance. (b) Linear combination fit of the total Auger spectrum (blue open circles) to normal (solid black line) and resonant (spectator + participator, green dashed line) components at 398 eV. (c) Linear combination fit for 398.3 eV. The fits in panels b and c demonstrate that the normal Auger component increases with higher photon energies, showing increasing rates of ultrafast intramolecular tunneling.

To get a sense for the time scales involved in electron tunneling in pure CuPC films, we have fit the total spectrum (blue open circles) to a linear combination of purely resonant (green dashed line) and normal Auger (solid black line) components, which is shown in Figure 4B and C for 398 and 398.3 eV, respectively. The purely resonant spectrum is taken as the Auger spectrum collected closest to the absorption edge (397.5 eV); the participator transition exhibits the largest intensity in this spectral region, corresponding to maximal localization of the core-excited electron. XAS transitions at energies above 398 eV correspond to excitation into progressively higher-lying unoccupied states. It is clear from the component fits in Figure 4B that already at the peak of the first π^* XAS resonance (398 eV), some fraction of electrons tunnel away from the core-hole on an ultrafast time scale. To quantify this delocalization, we have used integrated peak areas of the individual components to estimate ET times using

$$\frac{\tau_{\text{ET}}}{\tau_{\text{CH}}} = \frac{I_{\text{RA}}}{I_{\text{NA}}}$$

where τ_{ET} is the electron delocalization (transfer) time, τ_{CH} is the core-hole lifetime for N, and I_{NA} (I_{RA}) is the normal (resonant)

Auger intensity.¹¹ We estimate that at 398 eV, $\tau_{\text{ET}} = 40$ fs ($R^2 = 0.998$) and at 398.3 eV, $\tau_{\text{ET}} = 11$ fs ($R^2 = 0.995$). It should be noted that the 398.3 eV fit (Figure 4C) appears worse by eye, and this trend continues for higher energy excitations. We believe this is largely a consequence of (a) the energy dependence of the direct photoemission matrix elements, which have herein been assumed constant, and (b) difficulties associated with the identification of purely participator and purely spectator channels, (ignoring resonance detuning and associated dispersion as well as core-hole induced dynamics).^{6,7,11} However, the data clearly show that the delocalization time decreases (tunneling rate increases) at higher photon energies.

The fact that even for pure CuPC, electrons readily tunnel away from the core-hole adds complications to our efforts of extracting delocalization times for CuPC/ C_{60} interfaces as a function of photon energy. Thus, a single purely resonant CuPC spectrum near the absorption edge is insufficient to probe the energy-dependent electron transfer in our heterojunction films. This fact implies that we must use the total Auger spectrum of the pristine CuPC film at *different* photon energies (and not just near the absorption edge) to properly compare the bilayer films to CuPC-only films. At energies above the absorption edge, we have shown that the pure CuPC spectrum will necessarily contain both resonant (spectator + participator) and nonresonant (normal) Auger contributions. It follows that we are effectively estimating the *excess* tunneling due to intermolecular ET, i.e., that in addition to the intrinsic intramolecular delocalization of the pure CuPC.

Figure 5 shows RAE spectra for the multilayer CuPC/ C_{60} overlayer (face-on) sample for three photon energies close to the peak of the XAS resonance and the fits to the normal and resonant contributions. The overall shape is captured satisfactorily (although not perfectly), allowing us to estimate intermolecular ET times. As seen from the relative component contributions, the fraction of normal Auger grows monotonically for higher-lying excited states. The corresponding ET times are 61, 36, 17 fs, respectively (398.2, 398.45, 398.7 eV). Thus, the data show that compared to the pristine CuPC film, there is evidence for sub-100 fs electron delocalization to the C_{60} acceptor.

To compare ET dynamics between the two CuPC orientations relative to C_{60} , in Figure 6 we have plotted Auger spectra for the edge-on interface (submonolayer CuPC) at the same photon energies as the face-on case, along with the corresponding component fits. Due to the experimental geometry, the signal at 70 deg. incident angle for submonolayer edge-on CuPC samples is significantly smaller and hence noisier than the corresponding face-on case excited at 20 deg. incidence with its correspondingly larger excitation volume. We expect the error due to subtraction of the direct photoemission spectrum to be larger in the edge-on relative to the face-on case. These facts increase the fit uncertainty and make it more difficult to evaluate the branching ratio, especially for the highest photon energies. From inspection of the fits, it appears that the resonant component is underestimated, likely more so than in the face-on case. We find that at 398.2 eV, the fitted delocalization times between the two orientations do not differ within experimental error: 67 fs for edge-on vs 61 fs for face-on. Unlike in the face-on case, at 398.45 eV the total Auger spectrum is captured very well by a pure resonant spectrum, indicating no excess tunneling beyond the pure CuPC (intramolecular) case. For 398.7 eV, the estimated tunneling time is 53 fs, but this is likely a lower limit. Both ET time values are close to the limit of CHC, which is consistent with

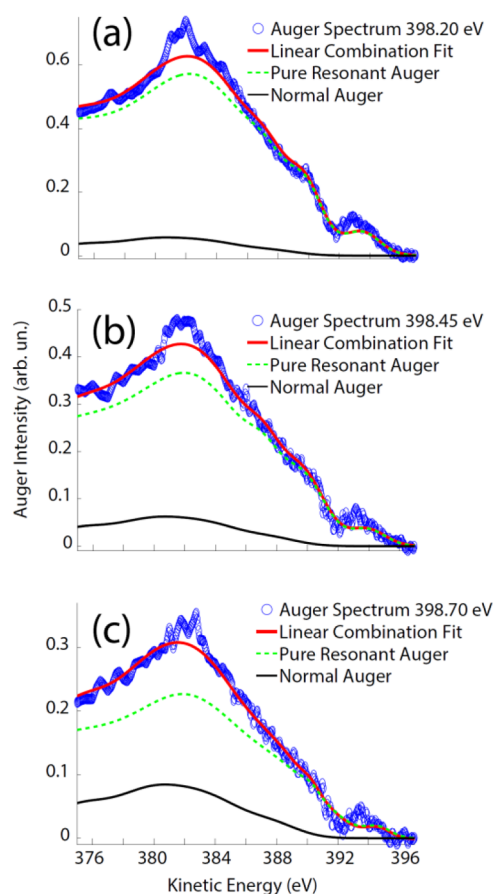


Figure 5. Auger linear combination fits for the face-on CuPc/C₆₀ heterojunction films for (a) 398.2 eV, (b) 398.45 eV, and (c) 398.7 eV. Since there is evidence for ultrafast intramolecular tunneling in pure CuPc films, we have used an Auger spectrum from pure CuPc at the corresponding photon energy to perform the linear combination fit for heterojunction films. Thus, the ratio of the normal Auger component of the heterojunction film and the resonant Auger spectrum of the pure CuPc film represents is used to estimate the excess intermolecular electron transfer to C₆₀ (additional to the intramolecular tunneling of pure CuPc). The spectral fits for this face-on interface suggest an increasing intermolecular ET rate with increasing photon energy. The delocalization times are 61, 36, and 17 fs for a, b, and c, respectively. The R^2 values for the fits for 398.2, 398.45, and 398.7 eV are 0.994, 0.994, and 0.994, respectively.

data from previous work on the dynamics of optical excited states at the edge-on CuPc/C₆₀ interface.^{16,17} The calculated lifetimes are summarized in Table 1.

We note that, as suggested by previous work, the high-energy shoulder of the first N K-edge XAS absorption feature likely contains a superposition of resonances corresponding to different initial and final states.^{18,19} That is, the spatial location of the N core-hole and the precise molecular orbital reached in the excitation may differ as a function of energy when one moves significantly off the main (low-energy) absorption peak. Therefore, for higher energy excitations at 398.7 eV, it is likely that final states are reached, whose wave functions qualitatively differ from the lower energy excitations. This is due to the fact that the excited electronic wavepacket evolves on a somewhat different potential energy surface;^{20–22} moreover, varying the excitation energy invariably leads to different vibrational transitions accompanying the electronic excitations. The net result of these considerations is that it is not immediately

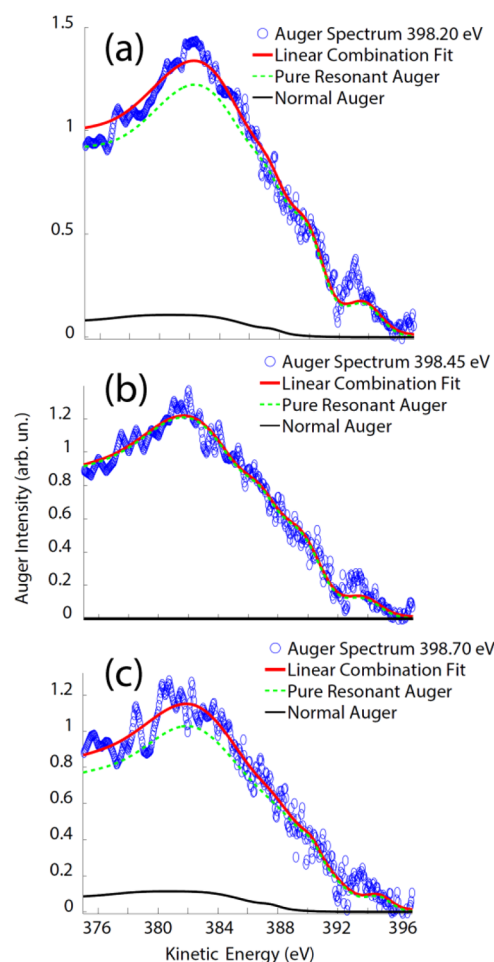


Figure 6. Linear combination fits for the edge-on CuPc/C₆₀ interface at the same photon energies as the corresponding face-on interface in Figure 4. Unlike the face-on case, the fits do not suggest the same trend of increasing tunneling time with photon energy. In fact, the resonant spectrum alone is sufficient to fit the total Auger spectrum at 398.45 eV. We estimate ET times of 67 and 53 fs for 398.2 (a) and 398.7 eV (c), respectively, with no evidence for intermolecular tunneling at 398.45 eV (b). The adjusted R^2 values are 0.986, 0.984, 0.972 for 398.2, 398.45, 398.7 eV, respectively.

Table 1. ET Times at Different Photon Energies for Face-On and Edge-On

sample	X-ray photon energy (eV)		
	398.20	398.45	398.70
HOPG/CuPc/C ₆₀ (face-on)	61 fs	36 fs	17 fs
HOPG/C ₆₀ /CuPc (edge-on)	67 fs	∞	53 fs

straightforward to relate the ET time scales at 398.7 eV to those at lower energy. Thus, we believe that care must be taken in interpreting the monotonic decrease in the ET time with increasing energy. However, since we expect the higher states and potential energy surface to be similar in the case of edge-on and face-on CuPc, the relative difference between the two orientations clearly suggests an enhanced ET rate in the case of the face-on interface.

Our results suggest that for higher-lying excited states, the interfacial D/A electronic coupling depends on the relative molecular orbital orientation. This agrees well with theoretical calculations from Bredas et al. on oriented pentacene/C₆₀

interfaces.²³ We note that estimates of the interfacial dipole yield a LUMO–LUMO offset between CuPc and C₆₀ that is ~2 times larger for the edge-on interface than the face-on case. Therefore, assuming comparable reorganization energies, the ET rate difference cannot be attributed to interface dipoles and corresponding difference in the driving force. We thus conclude that due to the enhanced molecular orbital overlap at the face-on oriented interface, the interfacial electronic coupling is larger when the π -electron densities on the donor and acceptor overlap relatively strongly.

We note that to make this determination, we have used the decay of core- π^* excitons to probe the ultrafast electron transfer dynamics and not the optically excited π - π^* excitonic states. Due to the difference in the localization radius of the hole wave function between these excited states, it is worth discussing the expected difference in the exciton binding energy. Although the perturbation due to the core-hole can be significant, we note that the report by Schnadt et al. has shown that in π -conjugated systems, the screening due to the polarizable π electrons is quite efficient, which makes the valence and core exciton binding energies quite comparable, though not identical (on the order of several hundred meV).²⁴ It is possible that the lowest energy excitation is lowered in energy due to core-hole relaxation so as to render the charge transfer to the (unperturbed) C₆₀ states energetically less favorable, localizing the exciting electron to give the longer charge transfer times observed in the experiment, and when this energetic hindrance is removed at higher energies, the difference in coupling can be observed. In addition, since one expects the core-hole induced effects to be primarily intramolecular and thus similar in both orientations, a relative comparison between interfacial orientations as presented is particularly favorable. Thus, even though the D/A coupling strength may not be identical for valence versus core excitons, we expect that the difference in the dynamics as a function of orientation in this study is directly relevant to the corresponding lower lying optical excitons.

Recently, there have been several reports of bilayer organic solar cell devices, where the donor was oriented face-on with respect to the acceptor and the substrate. The photocurrent was found to increase in the face-on relative to the edge-on case, which was attributed to a combination of increased absorption coefficients, an enhanced excitonic coupling, and a greater intermolecular charge transfer rate.⁴ Thus, in the face-on bilayer device, in addition to a strong donor/donor intermolecular coupling, as expected for a face-on π -stacked dimer, the interfacial D/A coupling is also significantly larger.

With further improvements in the exciton diffusion length (EDL) and absorption coefficients, such a bilayer architecture may hold promise for the future development of organic solar cells. However, even given a small EDL, strongly absorbing molecules like squaraine derivatives requiring ~10 nm thin films can in principle be oriented face-on with templating layers such as CuI.^{4,25} This will further raise both the absorption cross-section, the interfacial charge transfer rate, and potentially the out-of-plane charge hopping rates. Beyond implications for solar cells, our work contributes to the fundamental understanding of charge transfer processes in the condensed thin film state. Because the photon harvesting in its entirety inevitably depends on the competition between several rate processes, we believe our contribution makes clear that control of interfacial wave function overlap in the solid state constitutes a viable method to mediate these rates for optimal device function.

To summarize, we have used the CHC technique to investigate sub-100 fs electron transfer at model organic semiconductor heterointerfaces. To the best of our knowledge, this is the most relevant application of the CHC to measure ultrafast ET rates at organic/organic heterojunctions in the same geometry as the corresponding solar cell devices, taking full advantage of the elemental specificity of X-ray absorption. Our results suggest that the interfacial D/A electronic coupling is a function of the relative molecular orbital orientation. This in agreement with quantum chemical calculations on similar donor/acceptor interfaces. Our results underscore the need to control relative molecular orientation in thin solid films, and we believe that the face-on oriented interface can form the basis for efficient bilayer organic photovoltaics that could compete with the blend heterojunction approach for molecules with large absorption coefficients and/or large exciton diffusion lengths.

■ ASSOCIATED CONTENT

● Supporting Information

Detailed experimental and data reduction procedure, additional GIXD images, and a brief description of the Core–Hole Clock. This material is available free of charge via the Internet at <http://pubs.acs.org>.

■ AUTHOR INFORMATION

Corresponding Author

*E-mail: mftoney@slac.stanford.edu.

Present Address

|| (A.L.A.) Department of Chemistry and Biochemistry, University of California, Santa Cruz, Santa Cruz, CA 95064.

Notes

The authors declare no competing financial interest.

■ ACKNOWLEDGMENTS

This work was partially supported by the Center for Advanced Molecular Photovoltaics, Award No. KUS-C1-015-21, made by King Abdullah University of Science and Technology. We also acknowledge support from the Global Climate and Energy Program at Stanford. GIXD and X-ray spectroscopy measurements were carried out at the Stanford Synchrotron Radiation Lightsource, a national user facility operated by Stanford University on behalf of the U.S. Department of Energy, Office of Basic Energy Sciences. D.H.K acknowledges financial support by a grant (Code No. 2011-0031628) from the Center for Advanced Soft Electronics under the Global Frontier Research Program of the Ministry of Science, ICT and Future Planning, Korea.

■ REFERENCES

- (1) Deibel, C.; Strobel, T.; Dyakonov, V. Role of the Charge Transfer State in Organic Donor–Acceptor Solar Cells. *Adv. Mater.* **2010**, *22*, 4097–4111.
- (2) You, J.; Dou, L.; Yoshimura, K.; Kato, T.; Ohya, K.; Moriarty, T.; Emery, K.; Chen, C.-C.; Gao, J.; Li, G.; et al. A Polymer Tandem Solar Cell with 10.6% Power Conversion Efficiency. *Nat. Commun.* **2013**, *4*, 1446.
- (3) Heliatek Consolidates Its Technology Leadership by Establishing a New World Record for Organic Solar Technology with a Cell Efficiency of 12%. Heliatek Press Release, January 16, 2013 (http://www.heliatek.com/wp-content/uploads/2013/01/130116_PR_Heliatek_achieves_record_cell_efficiency_for_OPV.pdf).
- (4) Rand, B. P.; Cheyns, D.; Vasseur, K.; Giebink, N. C.; Mothy, S.; Yi, Y.; Coropceanu, V.; Beljonne, D.; Cornil, J.; Brédas, J.-L.; et al. The

Impact of Molecular Orientation on the Photovoltaic Properties of a Phthalocyanine/Fullerene Heterojunction. *Adv. Funct. Mater.* **2012**, *22*, 2987–2995.

(5) Guo, J.; Ohkita, H.; Bente, H.; Ito, S. Charge Generation and Recombination Dynamics in Poly(3-Hexylthiophene)/Fullerene Blend Films with Different Regioregularities and Morphologies. *J. Am. Chem. Soc.* **2010**, *132*, 6154–6164.

(6) Beye, M.; Föhlisch, A. Soft X-ray Probes of Ultrafast Dynamics for Heterogeneous Catalysis. *Chem. Phys.* **2013**, *414*, 130–138.

(7) Föhlisch, A.; Vijayalakshmi, S.; Pietzsch, A.; Nagasono, M.; Wurth, W.; Kirchmann, P. S.; Loukakos, P. A.; Bovensiepen, U.; Wolf, M.; Tchapyguine, M.; et al. Charge Transfer Dynamics in Molecular Solids and Adsorbates Driven by Local and Non-Local Excitations. *Surf. Sci.* **2012**, *606*, 881–885.

(8) Xiao, K.; Deng, W.; Keum, J. K.; Yoon, M.; Vlassioudis, I. V.; Clark, K. W.; Li, A.-P.; Kravchenko, I. I.; Gu, G.; Payzant, E. A.; et al. Surface-Induced Orientation Control of CuPc Molecules for the Epitaxial Growth of Highly Ordered Organic Crystals on Graphene. *J. Am. Chem. Soc.* **2013**, *135*, 3680–3687.

(9) Stohr, J.; Outka, A. Determination of Molecular Orientations on Surfaces from the Angular Dependence of Near-Edge X-ray Absorption Fine-Structure Spectra. *Phys. Rev. B* **1987**, *36*, 7891.

(10) Resel, R.; Ottmar, M.; Hanack, M.; Keckes, J.; Leising, G. Preferred Orientation of Copper Phthalocyanine Thin Films Evaporated on Amorphous Substrates. *J. Mater. Res.* **2011**, *15*, 934–939.

(11) Brühwiler, P. A.; Karis, O.; Mårtensson, N. Charge-Transfer Dynamics Studied Using Resonant Core Spectroscopies. *Rev. Mod. Phys.* **2002**, *74*, 703–740.

(12) Menzel, D. Ultrafast Charge Transfer at Surfaces Accessed by Core Electron Spectroscopies. *Chem. Soc. Rev.* **2008**, *37*, 2212–2223.

(13) Aristov, V. Y.; Molodtsova, O. V.; Maslyuk, V.; Vyalikh, D. V.; Zhilin, V. M.; Ossipyan, Y. A.; Bredow, T.; Mertig, I.; Knupfer, M. Electronic Structure of Pristine CuPc: Experiment and Calculations. *Appl. Surf. Sci.* **2007**, *254*, 20–25.

(14) Friedlein, R.; Sorensen, S.; Baev, A.; Gel'mukhanov, F.; Birgersson, J.; Crispin, A.; de Jong, M.; Osikowicz, W.; Murphy, C.; Ågren, H.; et al. Role of Electronic Localization and Charge-Vibrational Coupling in Resonant Photoelectron Spectra of Polymers: Application to Poly(paraphenylenevinylene). *Phys. Rev. B* **2004**, *69*, 125204.

(15) Beye, M.; Föhlisch, A. A Soft X-ray Approach to Electron–Phonon Interactions Beyond the Born–Oppenheimer Approximation. *J. Electron Spectrosc. Relat. Phenom.* **2011**, *184*, 313–317.

(16) Dutton, G.; Jin, W.; Reutt-Robey, J.; Robey, S. Ultrafast Charge-Transfer Processes at an Oriented Phthalocyanine/C₆₀ Interface. *Phys. Rev. B* **2010**, *82*, 073407.

(17) Kaake, L. G.; Barbara, P. F.; Zhu, X.-Y. Intrinsic Charge Trapping in Organic and Polymeric Semiconductors: A Physical Chemistry Perspective. *J. Phys. Chem. Lett.* **2010**, *1*, 628–635.

(18) Nardi, M. V.; Detto, F.; Aversa, L.; Verucchi, R.; Salvati, G.; Iannotta, S.; Casarin, M. Electronic Properties of CuPc and H₂Pc: An Experimental and Theoretical Study. *Phys. Chem. Chem. Phys.* **2013**, *15*, 12864–12881.

(19) Evangelista, F.; Carravetta, V.; Stefani, G.; Jansik, B.; Alagia, M.; Stranges, S.; Ruocco, A. Electronic Structure of Copper Phthalocyanine: An Experimental and Theoretical Study of Occupied and Unoccupied Levels. *J. Chem. Phys.* **2007**, *126*, 124709.

(20) Takahashi, O.; Odelius, M.; Nordlund, D.; Nilsson, A.; Bluhm, H.; Pettersson, L. G. M. Auger Decay Calculations with Core-Hole Excited-State Molecular-Dynamics Simulations of Water. *J. Chem. Phys.* **2006**, *124*, 64307.

(21) Hjelte, I.; Karlsson, L.; Svensson, S.; De Fanis, A.; Carravetta, V.; Saito, N.; Kitajima, M.; Tanaka, H.; Yoshida, H.; Hiraya, A.; et al. Angular Distribution of Different Vibrational Components of the X and B States Reached after Resonant Auger Decay of Core-Excited H₂O: Experiment and Theory. *J. Chem. Phys.* **2005**, *122*, 84306.

(22) Piancastelli, M. N.; Carravetta, V.; Hjelte, I.; De Fanis, A.; Okada, K.; Saito, N.; Kitajima, M.; Tanaka, H.; Ueda, K. Experimental and Theoretical Study of Resonant Auger Decay of Core-Excited NO₂. *Chem. Phys. Lett.* **2004**, *399*, 426–432.

(23) Yi, Y.; Coropceanu, V.; Brédas, J.-L. Exciton-Dissociation and Charge-Recombination Processes in Pentacene/C₆₀ Solar Cells: Theoretical Insight into the Impact of Interface Geometry. *J. Am. Chem. Soc.* **2009**, *131*, 15777–15783.

(24) Schnadt, J.; Schiessling, J.; Brühwiler, P. A. Comparison of the Size of Excitonic Effects in Molecular π Systems as Measured by Core and Valence Spectroscopies. *Chem. Phys.* **2005**, *312*, 39–45.

(25) Vasseur, K.; Broch, K.; Ayzner, A. L.; Rand, B. P.; Cheyns, D.; Frank, C.; Schreiber, F.; Toney, M. F.; Froyen, L.; Heremans, P. Controlling the Texture and Crystallinity of Evaporated Lead Phthalocyanine Thin Films for Near-Infrared Sensitive Solar Cells. *ACS Appl. Mater. Interfaces* **2013**, *5*, 8505–8515.